Technical note: Novel estimates of the leaf relative uptake rate of carbonyl sulfide from optimality theory

Georg Wohlfahrt[1], Albin Hammerle[1], Felix M. Spielmann[1], Florian Kitz[1], Chuixiang Yi[2,3]

[1]Department of Ecology, University of Innsbruck, Innsbruck, 6020, Austria
[2]School of Earth and Environmental Sciences, Queens College, City University of New York, New York 11367, USA.
[3]Earth and Environmental Sciences Department, Graduate Center, City University of New York, New York, NY 10016, USA.

Correspondence to: Georg Wohlfahrt (georg.wohlfahrt@uibk.ac.at)

Abstract. In order to estimate the gross primary productivity (GPP) of terrestrial ecosystems from the canopy uptake of carbonyl sulfide (COS), the leaf relative uptake rate (LRU) of COS with respect to carbon dioxide needs to be known *a priori*. Currently, the variability of the LRU between plant species in different biomes of the world is poorly understood, making the choice of an appropriate LRU uncertain and hampering further progress towards developing COS as a tracer of GPP. Here we propose a novel approach for estimating light-saturated LRU based on plant optimality principles, validate it against *in situ* leaf gas exchange measurements and provide global monthly climatological estimates. The global vegetation season average simulated LRUs fall into the 95 % range of 0.68-1.58 and are thus lower than most other published global estimates. We advocate these LRU estimates to be adopted by global modellers in order to test to what degree these are compatible with our current understanding of the sources and sinks in the global COS budget.

1 Introduction

The gross primary productivity (GPP) is a key conceptual term in the ecosystem carbon cycle, however cannot be directly measured at ecosystem-scale, requiring the application of indirect approaches based on the combination of proxy measurements and modelling (Wohlfahrt and Gu, 2015). During the last decade, carbonyl sulfide (COS) has emerged as a promising proxy for GPP, based on the observation that COS co-diffuses into plant leaves together with carbon dioxide (CO_2) during photosynthesis, but in contrast to the latter is not re-emitted (Sandoval-Soto et al., 2005).

The leaf relative uptake rate of COS with respect to CO_2, abbreviated as *LRU*, is instrumental to using COS as a proxy for GPP (Wohlfahrt et al., 2012). The *LRU* is the dimensionless ratio of the deposition velocities, that is the flux (F; pmol m^{-2} s^{-1} and µmol m^{-2} s^{-1}, respectively) normalized by the ambient (subscript *a*) mole fraction (C), of COS (superscript *s*; pmol mol^{-1}) with respect to CO_2 (superscript *c*; µmol mol^{-1}):

$$LRU = \frac{\frac{F^s}{C_a^s}}{\frac{F^c}{C_a^c}}. \quad (1)$$

Assuming negligible daytime mitochondrial leaf respiration (or accounting for it) allows replacing F^c with GPP and, provided *LRU* is known, rearrangement of Eq. (1) then yields a framework for estimating GPP based on measurements of C_a^c, C_a^s and F^s (Campbell et al., 2008):

$$GPP = F^s \frac{C_a^c}{C_a^s} LRU^{-1} . \quad (2)$$

Initial studies on the *LRU* suggested its value to gravitate to ca. 1.6 (Stimler et al., 2011; Stimler et al., 2010; Berkelhammer et al., 2014), a value which was successfully used by Asaf et al. (2013) in the first ever study that estimated ecosystem-scale GPP from corresponding COS flux measurements. The most recent review of published *LRU* values (Whelan et al., 2018) however indicates that, even though the median *LRU* amounts to 1.68, 95 % of the values fall into the range of 0.7 – 6.2, which is consistent with theoretical back-of-the-envelope calculations by Wohlfahrt et al. (2012). Here it should be noted that some of the higher values may result from measurements under low, non-saturating, light conditions, which are known to cause LRU to increase (Kooijmans et al., 2019). More recently, two field studies (Kooijmans et al., 2019; Sun et al., 2018) reported values around 1 under high incident photosynthetically active radiation (PAR).

Replacing the flux terms in Eq. (1) with the underlying Fick's diffusion equations (see Seibt et al., 2010 for a derivation), yields Eq. (3), which allows an assessment of the drivers underlying the *LRU*:

$$LRU = 1.21^{-1} \left(1 + \frac{g_s^s}{g_i^s}\right)^{-1} \left(1 - \frac{C_i^c}{C_a^c}\right)^{-1} , \quad (3)$$

where g_s^s and g_i^s represent the stomatal and internal, respectively, conductances to COS (mol m^{-2} s^{-1}), C_i^c the CO_2 mole fraction in the leaf intercellular space (µmol mol^{-1}) and the factor 1.21 converts the stomatal conductance to COS to its CO_2 counterpart. Note that the boundary layer conductances for COS and CO_2 have been assumed to be infinite here, as is typically the case in vigorously ventilated leaf chambers (Seibt et al., 2010). Eq. (3) shows the *LRU* to depend on two dimensionless ratios: (i) the stomatal-to-internal conductance to COS and (ii) the internal-to-ambient CO_2 mole fraction ratio. While the magnitude and drivers of g_i^s are poorly understood, g_s^s and $\frac{C_i^c}{C_a^c}$ are well known to vary over short timescales in response to diel changes in environmental drivers, as well as along large-scale bioclimatic gradients (Lloyd and Farquhar, 1994). With regard to the former, recent work by Kohonen et al. (2022) and Sun et al. (2022) demonstrated that contrasting leaf gas exchange theories are able to reproduce and explain the observed short-term response of *LRU* to key drivers such as incident PAR or the vapor pressure deficit (VPD).

In contrast, variability in *LRU* between biomes is poorly understood, partially due to a scarcity of measurements (Whelan et al., 2018), partially due to the lack of a suitable theoretical framework to predict *LRU a priori*, and the motivation for this work is thus to propose and apply a new theoretical approach for estimating large-scale bioclimatic patterns of *LRU*. To this end we make use of recent developments in plant optimality theory (Harrison et al., 2021).

2 Methods

2.1 Model theory

Here we use the P-model as described by Mengoli et al. (2022) and refer to this paper and references cited therein for further details. Briefly, the model, applicable only to C_3 plant species, is based on the combination of two optimality hypotheses – the least-cost and the coordination hypotheses. The least-cost hypothesis (Prentice et al., 2014) assumes that plants balance the carbon costs (per unit of photosynthesis) of maintaining the transpiration stream with those required for maintaining the carboxylation capacity and yields a $\frac{C_i^c}{C_a^c}$ ratio under which this balance is optimally realized:

$$\frac{C_i^c}{C_a^c} = \frac{\Gamma^*}{C_a^c} + \left(1 - \frac{\Gamma^*}{C_a^c}\right)\frac{\xi}{\xi+\sqrt{D}}, \text{ with} \quad (4)$$

$$\xi = \sqrt{\frac{\beta(K_m+\Gamma^*)}{1.6\eta^*}}. \quad (5)$$

Here Γ^*represents the CO_2 compensation point (Pa) in the absence of mitochondrial respiration, D the VPD (Pa), K_m the effective Michaelis-Menten coefficient of RUBISCO (Pa), $\eta^*$the dimensionless ratio of the viscosity of water at a given temperature to that at 25°C and β is a calibrated constant representing the ratio of the two cost terms. Wang et al. (2017b) calibrated β to a value of 146, based on their Table 1 we estimate a standard deviation for β of ± 18. ξ ($Pa^{0.5}$) represents the VPD response of the $\frac{C_i^c}{C_a^c}$ ratio. Eq. (4) has been successfully validated against global $\frac{C_i^c}{C_a^c}$ ratios derived from C^{13} isotope data by Wang et al. (2017b).

The coordination hypothesis (Maire et al., 2012) assumes that plants coordinate the investment of resources into electron transport and carboxylation capacity in a way such that photosynthesis, under average environmental conditions, is co-limited by the two and yields optimal values of the maximum carboxylation rate (V_{Cmax}; µmol m^{-2} s^{-1}) and the maximum electron transport rate (J_{max}; µmol m^{-2} s^{-1}):

$$V_{Cmax} = \varphi_o I \frac{C_i^c+K_m}{C_i^c+2\Gamma^*}\sqrt{1-\left[c^*\frac{C_i^c+2\Gamma^*}{C_i^c-\Gamma^*}\right]^{2/3}}, \text{ and} \quad (6)$$

$$J_{max} = \frac{4\varphi_o I}{\sqrt{\frac{1}{1-\left[c^*\frac{C_i^c+2\Gamma^*}{C_i^c-\Gamma^*}\right]^{2/3}}-1}}. \quad (7)$$

Here φ_o stands for the intrinsic quantum efficiency of photosynthesis (mol mol^{-1}), I represents absorbed PAR (µmol m^{-2} s^{-1}) and c^* is a calibrated (0.41) dimensionless cost factor for electron transport. V_{Cmax} was successfully validated against corresponding leaf gas exchange measurements by Smith et al. (2019).

Usually, absorbed PAR in Eq. (7) is derived by multiplying the incident PAR with the (satellite-derived) fraction of absorbed PAR (fAPAR) as a simple means of leaf-to-canopy scaling (Stocker et al., 2020). Here, in order to compare to the available *LRU* studies and in order to avoid the complexities of leaf to canopy scaling, the main interest is in the leaf-scale and the P-model was thus driven by incident PAR (leaf absorptance of PAR is included in the value of φ_o). Model simulations can thus be thought to represent leaves at the top of the plant canopy.

V_{Cmax} and J_{max}, together with the optimal $\frac{c_i^c}{c_a^c}$ ratio, allow estimating GPP via the familiar FvCB photosynthesis model (Farquhar et al., 1980) and applying Fick's law in turn yields g_s^c and thus g_s^s. Finally, g_i^s is obtained by scaling it to V_{Cmax}, as first proposed by Berry et al. (2013):

$$g_i^s = \alpha V_{Cmax} \, . \tag{8}$$

The parameter α was calibrated to 1200e^{-6} for C_3 species by Berry et al. (2013), here we use the more recent value of 1616e^{-6} ± 562e^{-6} derived by Kooijmans et al. (2021) through calibration of the SiB4 model against ecosystem-scale flux observations. Together, Eqs. (4-8) with the five environmental inputs temperature, VPD, PAR, C_a^c, and air pressure, allow calculating the *LRU* via Eq. (3).

The optimality implied in the P-model is likely to operate on multi-day to weekly time scales, as plants acclimate to the prevailing environmental conditions. Mengoli et al. (2022) thus devised an approach in which optimal (acclimated) values of ξ, V_{Cmax} and J_{max} are calculated as running averages over a defined antecedent period. They show that a 15-day moving average over midday hours produces the best correspondence with empirical GPP derived from eddy covariance CO_2 flux measurements. We follow their approach, but recognize that this may be cause a bias in situations when the peak of GPP occurs outside of this time window, e.g. in the case of drought stress. For short-term, e.g. hourly, simulations, the acclimated values are then adjusted to the current environmental conditions on the basis of which instantaneous values of GPP, g_s^c, and the $\frac{c_i^c}{c_a^c}$ ratio are finally calculated.

2.2 Data and model application

For validation we retrieved the datasets underlying the work by Kooijmans et al. (2019) and Sun et al. (2018) from the associated data repositories. Kooijmans et al. (2019) investigated the leaf-scale COS exchange of Scots pine (*Pinus sylvestris*) at the study site Hyytiälä in Finland (61°51′ N, 24°17′ E) using two independent chambers, while Sun et al. (2018) studied the leaf-scale COS exchange of broadleaf cattail (*Typha latifolia*) at the San Joaquin freshwater marsh site in California/USA (33° 39′ N, 117° 51′ W). The major environmental difference between both studies is air temperature, which was ca. 7°C and 22°C during the study period of Kooijmans et al. (2019) and Sun et al. (2018), respectively. The latter dataset did not include air pressure, which was inferred from elevation using the equation implemented in the P-model (Wang et al., 2017a). Given that the large-scale bioclimatic patterns of *LRU*, rather than its short-term variability, are the central interest of this paper, all model

output was filtered for PAR > 1000 µmol m^{-2} s^{-1} in order to assure light saturation. Validation statistics include the mean bias error (MBE), the root mean squared error (RMSE) and the coefficient of determination (R^2).

For application at the global scale, we calculated monthly climatologies of all inputs for the period 2001-2010 at a 0.05° resolution assuming that plants would fully acclimate to the environmental conditions at this time scale. By virtue of the coordination hypothesis (Maire et al., 2012), photosynthesis under these conditions is assumed to be co-limited by electron transport and the activity of Rubisco and thus light-saturated. Air temperature and VPD were taken from the Chelsea repository (version 2.1; Karger et al., 2018; Karger et al., 2017), incident PAR from Ryu et al. (2018), ambient CO_2 mole fractions from Cheng et al. (2022) and pressure was derived from a global digital elevation model included in the Chelsea repository using the equation implemented in the P-model (Wang et al., 2017a).

The *LRU* calculated with the P-model is sensitive to two calibrated parameters, α and β in Eqs. (5) and (8), respectively. A sensitivity analysis was carried out by independently changing their default values (see above) by ± one standard deviation (see above) and averaging the resulting absolute differences to the *LRU* calculated with the default value. The simulated *LRU* is not sensitive to c^*, the dimensionless cost factor for electron transport, which affects both V_{Cmax} and J_{max} through Eqs. (6) and (7). Changes in these two parameters propagate to g_s^s, however because the changes in V_{Cmax} and g_s^s are proportional, the ratio of g_s^s to g_i^s and thus *LRU* (Eq. 3) are unaffected by changes in c^*.

3 Results and Discussion

As shown in Fig. 1, Eq. (3) fed with inputs from the P-model overestimates the LRU of *Typha latifolia* (MBE: 0.53, RMSE: 0.59), while the *LRU* of *Pinus sylvestris* is underestimated (MBE: -0.54 and -0.64 for chamber #1 and #2, respectively, RMSE: 0.72 and 1.03 for chamber #1 and #2, respectively). The model also underestimates the variability in measured *LRU*, resulting poor R^2 values (*Typha latifolia*: 0.01, *Pinus sylvestris*: 0.03 and 0.11 for chamber #1 and #2, respectively). While the P-model, or its predecessors, have been successfully validated in terms of the $\frac{c_i^c}{c_a^c}$ ratio and V_{Cmax} (Smith et al., 2019; Wang et al., 2017b), validation of *LRU* thus remains inconclusive and points to the urgent need for more *in situ* leaf gas exchange measurements from the major biomes of the world in order to truly understand to what degree the model is capable of reproducing the global patterns of *LRU*.

In order to exemplify the application of the model at global scale, Fig. 2 shows a global map of the growing season average *LRU*. Simulated *LRUs*, exclusive of pixels with a C_4 fractional cover > 50 %, reach low values around 0.62 in the higher latitudes and, with a longitudinal mean of 1.57, peak in the tropics. The global median *LRU* amounts to 0.90, with a 95 % range of 0.68-1.58, and is thus for most part lower than the median value (1.68) compiled in the recent review by Whelan et

al. (2018). Figure 3 shows that the *LRU* values of this study are lower than those compiled by Seibt et al. (2010) and Whelan et al. (2018) across all plant functional types (PFTs). These two studies however did not filter for high radiation which may, because *LRU* increases at low PAR values (e.g. Kooijmans et al., 2019; Sun et al., 2018), at least partly explain the difference. Our values are also lower (by up to 26 %) across all PFTs, except the Boreal needleleaf summergreen and the Temperate broadleaf evergreen forest PFTs, compared to those reported recently by Maignan et al. (2021), who used the output of the process-based ORCHIDEE model to back-calculate global *LRUs*. In this comparison it should be noted that ORCHIDEE integrates LRU over the depth of the plant canopy. PAR availability, together with VPD the major driver of short-term variability in *LRU*, typically decrease with canopy depth and since *LRU* is negatively related to PAR (e.g. Kooijmans et al., 2019; Kohonen et al., 2022), canopy-integrated *LRU* is expected to be larger than leaf-scale *LRU* at the top of the canopy (Sun et al., 2022). This in turn suggests the difference to the values by Maignan et al. (2021) to diminish if their values were expressed at leaf-scale and top of the canopy environmental conditions. Possibly, this scaling effect may explain the increasing bias from boreal over temperate to tropical PFTs (Fig. 3). Despite this issue, the *LRU*s by Maignan et al. (2021) and this study are highly correlated across PFTs ($R^2 > 0.93$, Fig. 3), suggesting that both approaches reproduce similar patterns across the global bioclimatic space even though using contrasting modelling approaches. Stomatal conductance in the ORCHIDEE model is prescribed to be linearly related to GPP based on Yin and Struik (2009), the P-model, in contrast, employs an optimality approach (Mengoli et al., 2022). In addition, the ORCHIDEE model uses parameters specific to plant functional types, while P-model parameters are globally invariant.

It remains to be seen whether our, compared to previous estimates, low *LRU* values are able to resolve the longstanding conundrum in the global atmospheric COS budget, which is that estimates of a large land COS sink require an upward-tweak of the ocean source for the budget to close (Whelan et al., 2018). The magnitude of the required increases in the ocean source are however at odds with bottom-up estimates (Lennartz et al., 2017; Lennartz et al., 2021).

A sensitivity analysis of the two major model parameters, α and β, shown in Fig. 4, suggests that the simulated growing season averaged *LRU* is most sensitive to uncertainty in α, which scales g_i^s to V_{Cmax}. A change in α by ± one standard deviation causes a change in *LRU* between 15-27 %, the largest changes occurring in the mid to high northern latitudes. This indicates an urgent need for more data in order to better constrain g_i^s via Eq. (8) and also continuing efforts towards improving our process understanding of the drivers of g_i^s, as Berry et al. (2013) noted that Eq. (8) is poorly constrained by data. In contrast, a change in β by ± one standard deviation causes a maximum change in LRU of 2 %, the largest effect being observed in the tropics.

4 Conclusions

Accurate knowledge of the *LRU* is prerequisite to using Eq. (2) for estimating GPP (Wohlfahrt et al., 2012). While earlier work suggested the *LRU*, under saturating light conditions, to be confined to ca. 1.6 (Stimler et al., 2011; Stimler et al., 2010;

Berkelhammer et al., 2014), current cumulative evidence suggests the *LRU* to be more variable (Whelan et al., 2018) and Sun et al. (2022) recently concluded from a theoretical analysis "there is no guarantee for *LRU* to converge to a narrow range across species". Inspection of Eq. (3) shows that convergence to a universal value would require the $\frac{C_i^c}{C_a^c}$ and $\frac{g_s^s}{g_i^s}$ ratios to be constant or compensating changes between the two. At present we have no evidence to support either of these scenarios. Rather, our global simulations, based on plant optimality principles, suggest the *LRU* to predictably vary (Fig. 2), reflecting spatial patterns in the $\frac{C_i^c}{C_a^c}$ ratio, g_s^s and g_i^s (Supplemental Fig. S1). We recognize that our values, in the range between 0.6 and 2.2, are low compared to those used in previous global assessments (Figs. 2 and 3). We thus advocate, until more empirical measurements become available for validating our simulations, forward and inverse modellers to adopt our values/approach in order to examine whether these help to reconcile some of the long-standing inconsistencies in the global COS budget.

Code and data availability:

The datasets of Kooijmans et al. (2019) and Sun et al. (2018) are available from https://zenodo.org/record/1211481#.Y0VnjC-2276 and https://datadryad.org/stash/dataset/doi:10.15146/R37T00, respectively. Air temperature, VPD and the digital elevation model were taken from https://chelsa-climate.org, incident PAR from https://www.environment.snu.ac.kr/bess-rad, CO_2 mole fractions from https://zenodo.org/record/5021361#.Y0Vmz0zP2gM. All data and the Matlab scripts used for processing these and creating the figures can be found at https://doi.org/10.5281/zenodo.7185591. For easy adoption of our global LRUs by modellers we provide these as monthly climatological means, averaged for the period 2001-2010, at 0.05° resolution (lru_pmodel_global_monthly_climatology_v02.nc).

Author contributions:

GW conceived the study and conducted the simulations and analyses with the help of AH. All authors contributed to the writing of the manuscript.

Competing interests:

The authors declare no competing interests.

Acknowledgements:

The authors thank Colin Prentice and Julia Mengoli for patiently answering questions regarding the P-model. Fabienne Maignan and Camille Abadie are acknowledged for providing the ORCHIDEE plant functional type map. Figures 3 and 4 as well as Supplemental Figure S1 use colormaps provided by Crameri (2018).

Financial support:

This study was financially supported by the Austrian Science Fund (FWF) through grant P35737.

References

Asaf, D., Rotenberg, E., Tatarinov, F., Dicken, U., Montzka, S. A., and Yakir, D.: Ecosystem photosynthesis inferred from measurements of carbonyl sulphide flux, Nat. Geosci., 6, 186–190, 10.1038/ngeo1730, 2013.

Berkelhammer, M., Asaf, D., Still, C., Montzka, S., Noone, D., Gupta, M., Provencal, R., Chen, H., and Yakir, D.: Constraining surface carbon fluxes using in situ measurements of carbonyl sulfide and carbon dioxide, Global Biogeochemical Cycles, 28, 161-179, 10.1002/2013GB004644, 2014.

Berry, J., Wolf, A., Campbell, J. E., Baker, I., Blake, N., Blake, D., Denning, A. S., Kawa, S. R., Montzka, S. A., Seibt, U., Stimler, K., Yakir, D., and Zhu, Z.: A coupled model of the global cycles of carbonyl sulfide and CO_2: A possible new window on the carbon cycle, Journal of Geophysical Research: Biogeosciences, 118, 842-852, 10.1002/jgrg.20068, 2013.

Campbell, J. E., Carmichael, G. R., Chai, T., Mena-Carrasco, M., Tang, Y., Blake, D. R., Blake, N. J., Vay, S. A., Collatz, G. J., Baker, I., Berry, J. A., Montzka, S. A., Sweeney, C., Schnoor, J. L., and Stanier, C. O.: Photosynthetic control of atmospheric carbonyl sulfide during the growing season, Science, 322, 1085-1088, 10.1126/science.1164015, 2008.

Cheng, W., Dan, L., Deng, X., Feng, J., Wang, Y., Peng, J., Tian, J., Qi, W., Liu, Z., Zheng, X., Zhou, D., Jiang, S., Zhao, H., and Wang, X.: Global monthly gridded atmospheric carbon dioxide concentrations under the historical and future scenarios, Scientific Data, 9, 83, 10.1038/s41597-022-01196-7, 2022.

Crameri, F.: Scientific colour maps [dataset], 10.5281/zenodo.1243862, 2018.

Farquhar, G. D., Caemmerer, S., and Berry, J. A.: A biochemical model of photosynthetic CO_2 assimilation in leaves of C_3 species, Planta, 149, 78-90, 10.1007/BF00386231, 1980.

Harrison, S. P., Cramer, W., Franklin, O., Prentice, I. C., Wang, H., Brännström, Å., de Boer, H., Dieckmann, U., Joshi, J., Keenan, T. F., Lavergne, A., Manzoni, S., Mengoli, G., Morfopoulos, C., Peñuelas, J., Pietsch, S., Rebel, K. T., Ryu, Y., Smith, N. G., Stocker, B. D., and Wright, I. J.: Eco-evolutionary optimality as a means to improve vegetation and land-surface models, New Phytol., 10.1111/nph.17558, 2021.

Karger, D. N., Conrad, O. B., J. , Kawohl, T., Kreft, H., Soria-Auza, R. W. Z., N. E., and Linder, H. P. K., M.: Data from: Climatologies at high resolution for the earth's land surface areas, DRYAD [dataset], 10.5061/dryad.kd1d4, 2018.

Karger, D. N., Conrad, O., Bohner, J., Kawohl, T., Kreft, H., Soria-Auza, R. W., Zimmermann, N. E., Linder, H. P., and Kessler, M.: Climatologies at high resolution for the earth's land surface areas, Scientific Data, 4, 170122, 10.1038/sdata.2017.122, 2017.

Kohonen, K.-M., Dewar, R., Tramontana, G., Mauranen, A., Kolari, P., Kooijmans, L. M. J., Papale, D., Vesala, T., and Mammarella, I.: Intercomparison of methods to estimate gross primary production based on CO2 and COS flux measurements, Biogeosciences, 19, 4067-4088, 10.5194/bg-19-4067-2022, 2022.

Kooijmans, L. M. J., Sun, W., Aalto, J., Erkkila, K. M., Maseyk, K., Seibt, U., Vesala, T., Mammarella, I., and Chen, H.: Influences of light and humidity on carbonyl sulfide-based estimates of photosynthesis, Proc. Natl. Acad. Sci. U.S.A., 10.1073/pnas.1807600116, 2019.

Kooijmans, L. M. J., Cho, A., Ma, J., Kaushik, A., Haynes, K. D., Baker, I., Luijkx, I. T., Groenink, M., Peters, W., Miller, J. B., Berry, J. A., Ogée, J., Meredith, L. K., Sun, W., Kohonen, K.-M., Vesala, T., Mammarella, I., Chen, H., Spielmann, F. M., Wohlfahrt, G., Berkelhammer, M., Whelan, M. E., Maseyk, K., Seibt, U., Commane, R., Wehr, R., and Krol, M.: Evaluation of carbonyl sulfide biosphere exchange in the Simple Biosphere Model (SiB4), Biogeosciences, 18, 6547-6565, 10.5194/bg-18-6547-2021, 2021.

Krinner, G., Viovy, N., de Noblet-Ducoudré, N., Ogée, J., Polcher, J., Friedlingstein, P., Ciais, P., Sitch, S., and Prentice, I. C.: A dynamic global vegetation model for studies of the coupled atmosphere-biosphere system, Global Biogeochemical Cycles, 19, 10.1029/2003GB002199, 2005.

Lennartz, S. T., Gauss, M., von Hobe, M., and Marandino, C. A.: Monthly resolved modelled oceanic emissions of carbonyl sulphide and carbon disulphide for the period 2000–2019, Earth System Science Data, 13, 2095-2110, 10.5194/essd-13-2095-2021, 2021.

Lennartz, S. T., Marandino, C. A., von Hobe, M., Cortes, P., Quack, B., Simo, R., Booge, D., Pozzer, A., Steinhoff, T., Arevalo-Martinez, D. L., Kloss, C., Bracher, A., Röttgers, R., Atlas, E., and Krüger, K.: Direct oceanic emissions unlikely to account for the missing source of atmospheric carbonyl sulfide, Atmospheric Chemistry and Physics, 17, 385-402, 10.5194/acp-17-385-2017, 2017.

Lloyd, J. and Farquhar, G.: ^{13}C discrimination during CO_2 assimilation by the terrestrial biosphere, Oecologia, 99, 201-215, 10.1007/BF00627732, 1994.

Maignan, F., Abadie, C., Remaud, M., Kooijmans, L. M. J., Kohonen, K.-M., Commane, R., Wehr, R., Campbell, J. E., Belviso, S., Montzka, S. A., Raoult, N., Seibt, U., Shiga, Y. P., Vuichard, N., Whelan, M. E., and Peylin, P.: Carbonyl sulfide: comparing a mechanistic representation of the vegetation uptake in a land surface model and the leaf relative uptake approach, Biogeosciences, 18, 2917-2955, 10.5194/bg-18-2917-2021, 2021.

Maire, V., Martre, P., Kattge, J., Gastal, F., Esser, G., Fontaine, S., and Soussana, J. F.: The coordination of leaf photosynthesis links C and N fluxes in C_3 plant species, PLoS One, 7, e38345, 10.1371/journal.pone.0038345, 2012.

Mengoli, G., Agustí-Panareda, A., Boussetta, S., Harrison, S. P., Trotta, C., and Prentice, I. C.: Ecosystem Photosynthesis in Land-Surface Models: A First-Principles Approach Incorporating Acclimation, Journal of Advances in Modeling Earth Systems, 14, 10.1029/2021ms002767, 2022.

Prentice, I. C., Dong, N., Gleason, S. M., Maire, V., and Wright, I. J.: Balancing the costs of carbon gain and water transport: testing a new theoretical framework for plant functional ecology, Ecol. Lett., 17, 82-91, 10.1111/ele.12211, 2014.

Ryu, Y., Jiang, C., Kobayashi, H., and Detto, M.: MODIS-derived global land products of shortwave radiation and diffuse and total photosynthetically active radiation at 5 km resolution from 2000, Remote Sens. Environ., 204, 812-825, 10.1016/j.rse.2017.09.021, 2018.

Sandoval-Soto, L., Stanimirov, M., von Hobe, M., Schmitt, V., Valdes, J., Wild, A., and Kesselmeier, J.: Global uptake of carbonyl sulfide (COS) by terrestrial vegetation: Estimates corrected by deposition velocities normalized to the uptake of carbon dioxide (CO_2), Biogeosciences, 2, 125-132, 10.5194/bg-2-125-2005, 2005.

Seibt, U., Kesselmeier, J., Sandoval-Soto, L., Kuhn, U., and Berry, J. A.: A kinetic analysis of leaf uptake of COS and its relation to transpiration, photosynthesis and carbon isotope fractionation, Biogeosciences, 7, 333-341, 10.5194/bg-7-333-2010, 2010.

Smith, N. G., Keenan, T. F., Colin Prentice, I., Wang, H., Wright, I. J., Niinemets, U., Crous, K. Y., Domingues, T. F., Guerrieri, R., Yoko Ishida, F., Kattge, J., Kruger, E. L., Maire, V., Rogers, A., Serbin, S. P., Tarvainen, L., Togashi, H. F., Townsend, P. A., Wang, M., Weerasinghe, L. K., and Zhou, S. X.: Global photosynthetic capacity is optimized to the environment, Ecol. Lett., 10.1111/ele.13210, 2019.

Stimler, K., Berry, J. A., Montzka, S. A., and Yakir, D.: Association between Carbonyl Sulfide Uptake and $^{18}\Delta$ during Gas Exchange in C_3 and C_4 Leaves, Plant Physiology, 157, 509-517, 10.1104/pp.111.176578, 2011.

Stimler, K., Montzka, S. A., Berry, J. A., Rudich, Y., and Yakir, D.: Relationships between carbonyl sulfide (COS) and CO_2 during leaf gas exchange, New Phytol., 186, 869-878, 10.1111/j.1469-8137.2010.03218.x, 2010.

Stocker, B. D., Wang, H., Smith, N. G., Harrison, S. P., Keenan, T. F., Sandoval, D., Davis, T., and Prentice, I. C.: P-model v1.0: an optimality-based light use efficiency model for simulating ecosystem gross primary production, Geoscientific Model Development, 13, 1545-1581, 10.5194/gmd-13-1545-2020, 2020.

Sun, W., Berry, J. A., Yakir, D., and Seibt, U.: Leaf relative uptake of carbonyl sulfide to CO_2 seen through the lens of stomatal conductance-photosynthesis coupling, New Phytol., 235, 1729-1742, 10.1111/nph.18178, 2022.

Sun, W., Maseyk, K., Lett, C., and Seibt, U.: Stomatal control of leaf fluxes of carbonyl sulfide and CO_2 in a *Typha* freshwater marsh, Biogeosciences, 15, 3277-3291, 10.5194/bg-15-3277-2018, 2018.

Wang, H., Prentice, I. C., Davis, T. W., Keenan, T. F., Wright, I. J., and Peng, C.: Photosynthetic responses to altitude: an explanation based on optimality principles, New Phytol., 213, 976-982, 10.1111/nph.14332, 2017a.

Wang, H., Prentice, I. C., Keenan, T. F., Davis, T. W., Wright, I. J., Cornwell, W. K., Evans, B. J., and Peng, C.: Towards a universal model for carbon dioxide uptake by plants, Nature Plants, 3, 734-741, 10.1038/s41477-017-0006-8, 2017b.

Whelan, M. E., Lennartz, S. T., Gimeno, T. E., Wehr, R., Wohlfahrt, G., Wang, Y., Kooijmans, L. M. J., Hilton, T. W., Belviso, S., Peylin, P., Commane, R., Sun, W., Chen, H., Kuai, L., Mammarella, I., Maseyk, K., Berkelhammer, M., Li, K.-F., Yakir, D., Zumkehr, A., Katayama, Y., Ogée, J., Spielmann, F. M., Kitz, F., Rastogi, B., Kesselmeier, J., Marshall, J., Erkkilä, K.-M., Wingate, L., Meredith, L. K., He, W., Bunk, R., Launois, T., Vesala, T., Schmidt, J. A., Fichot, C. G., Seibt, U., Saleska, S., Saltzman, E. S., Montzka, S. A., Berry, J. A., and Campbell, J. E.: Reviews and syntheses: Carbonyl sulfide as a multi-scale tracer for carbon and water cycles, Biogeosciences, 15, 3625-3657, 10.5194/bg-15-3625-2018, 2018.

Wohlfahrt, G. and Gu, L.: The many meanings of gross photosynthesis and their implication for photosynthesis research from leaf to globe, Plant Cell Environ., 38, 2500-2507, 10.1111/pce.12569, 2015.

Wohlfahrt, G., Brilli, F., Hoertnagl, L., Xu, X., Bingemer, H., Hansel, A., and Loreto, F.: Carbonyl sulfide (COS) as a tracer for canopy photosynthesis, transpiration and stomatal conductance: potential and limitations, Plant Cell Environ., 35, 657-667, 10.1111/j.1365-3040.2011.02451.x, 2012.

Yin, X. and Struik, P. C.: C_3 and C_4 photosynthesis models: An overview from the perspective of crop modelling, NJAS - Wageningen Journal of Life Sciences, 57, 27-38, 10.1016/j.njas.2009.07.001, 2009.

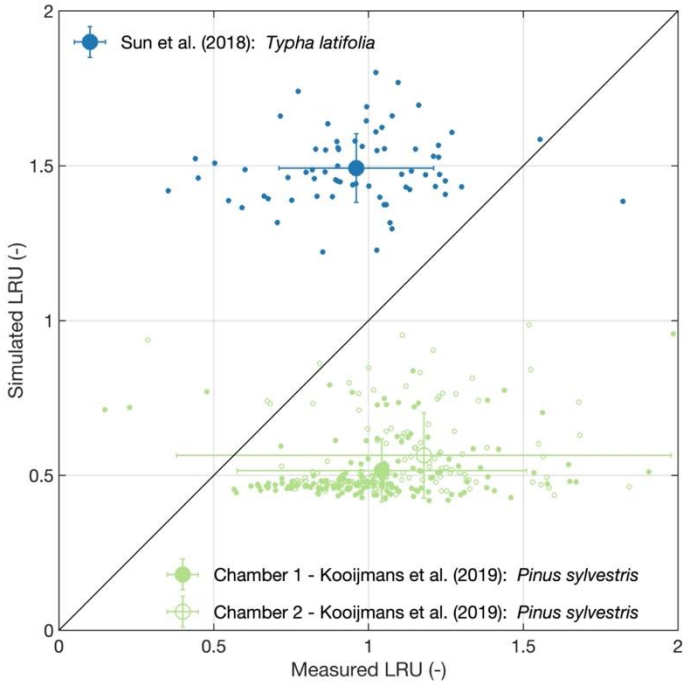

Figure 1: Model validation. Large symbols and error bars represent means and their standard deviations, respectively, while small symbols refer to raw data.

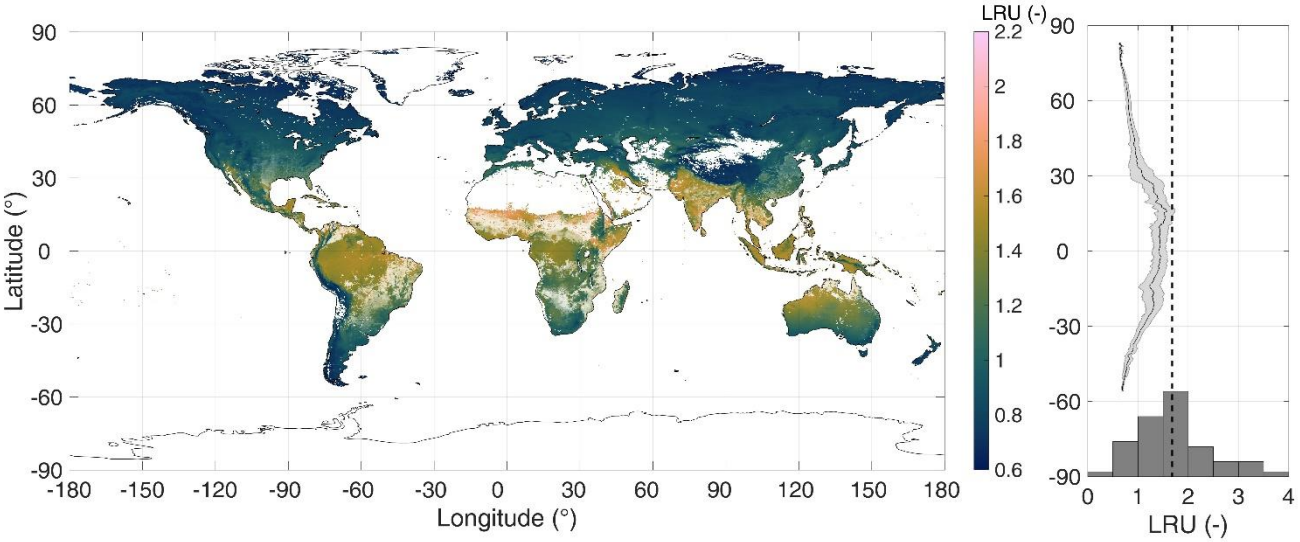

Figure 2: Simulated growing season (monthly average air temperature above 0°C) average global LRU (left panel) and longitudinal averages (right panel). The C_4 plant cover fraction is indicated by the transparency level of the color coding. In the right panel, the solid line and the shaded area represent longitudinal means and their standard deviations, respectively, omitting pixels where the C_4 plant cover fraction exceeds 50 %. The histogram in the right panel shows the data of C_3 species from Figure 2 in Whelan et al. (2018; omitting 4 data points with LRU > 4); the dashed line represents the median (1.68) LRU of C_3 species from Whelan et al. (2018).

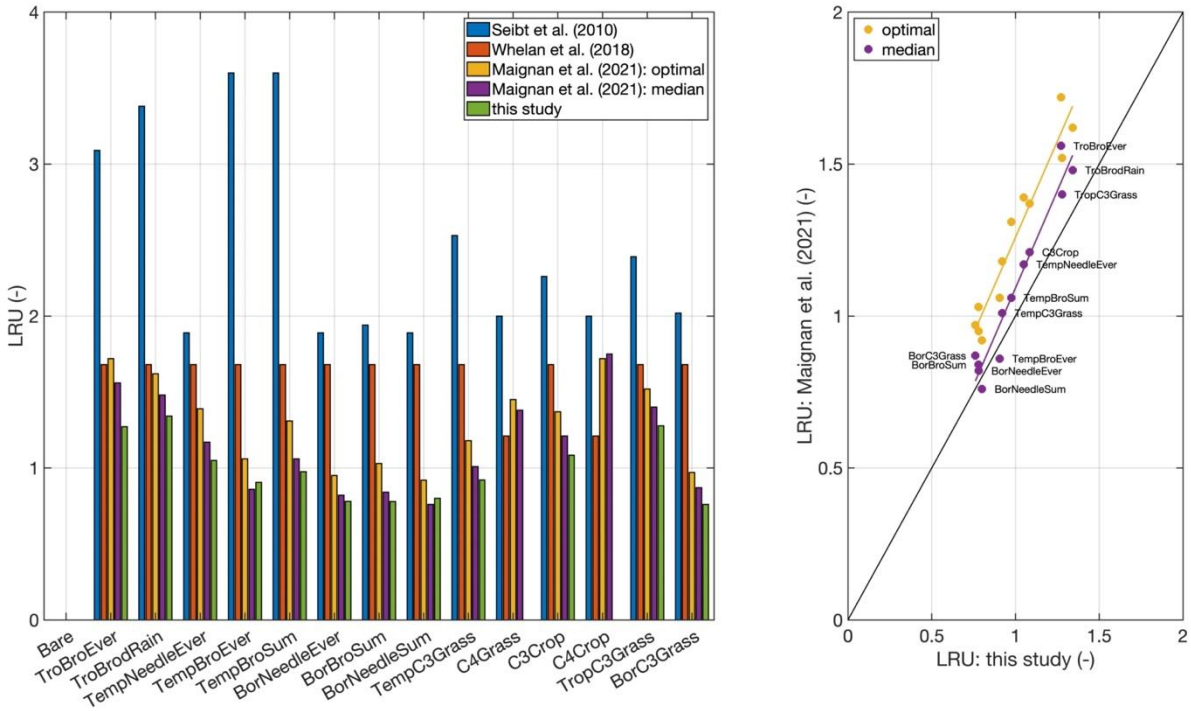

Figure 3: Comparison to published global LRU values averaged by plant functional type. Published LRU values were taken from Table 1 in Maignan et al. (2021). The plant functional type classification corresponds to the one used in the ORCHIDEE model (Krinner et al., 2005). No values are given for the C_4 grass and crop plant functional types, since the model is applicable to C_3 species only. The right panel shows a scatter plot of the LRUs from this study and the two versions reported by Maignan et al. (2021).

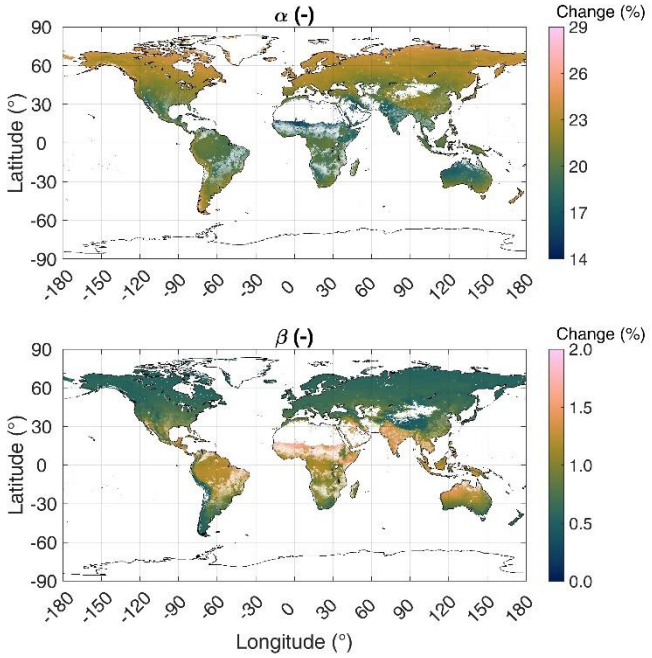

Figure 4: Sensitivity of simulated growing season average (defined as monthly air temperature > 0°C) LRU to changing parameters α (upper panel) and β (lower panel) by ± one standard deviation. The C_4 plant cover fraction is indicated by the transparency level of the color coding.